Hindawi Publishing Corporation
International Journal of Mathematics and Mathematical Sciences
Volume 2008, Article ID 474782, 21 pages
doi:10.1155/2008/474782

Research Article

Discrete Dynamics by Different Concepts of Majorization

S. Sauerbrei, P. J. Plath, and M. Eiswirth

Fritz-Haber-Institut der Max-Planck-Gesellschaft, Faradayweg 4-6, 14195 Berlin, Germany

Correspondence should be addressed to S. Sauerbrei, sonja@fhi-berlin.mpg.de

Received 6 May 2008; Accepted 19 June 2008

Recommended by Andrei Volodin

For the description of complex dynamics of open systems, an approach is given by different concepts of majorization (order structure). Discrete diffusion processes with both invariant object number and sink or source can be represented by the development of Young diagrams on lattices. As an experimental example, we investigated foam decay, dominated by sinks. The relevance of order structures for the characterization of certain processes is discussed.

1. Introduction

The concept of majorization (order structure) goes back to Hardy et al. [1, 2] and was investigated by Uhlmann and Alberti [3–6], and Marshall and Olkin [7] in detail. Majorization plays an important role in quantum information theory; see Nielsen [8].

This mathematical concept offers, by various extensions, many ways for the description of discrete process dynamics. One of these extensions enables the inclusion of a sink (weak submajorization [7]) or a source (weak supermajorization [7]) for objects during the process dynamics.

A description of special processes by majorization was developed by Zylka [9–12]. He defined an attainability of states. By equalizing processes a set of attainable states, which belongs to an initial state, forms a complicated geometrical structure in state spaces. These structures are polyhedra which are in general nonconvex.

A discrete majorization can be represented by diagram lattices (lattices of Young diagrams [13, 14]) which were introduced by Ruch [15]. The lattice structures lead to a description of elementary transitions for both discrete classical and discrete weak majorizations. A representation of sets of attainability by lattices is also possible.

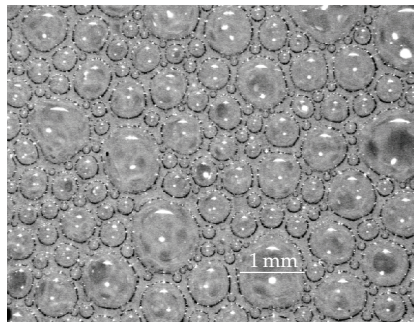

Figure 1: A foam image at 190 seconds.

Another variant of majorization can be formulated by taking into account permutations. In [16], we investigated the structures and lattices of Young diagrams and their permutations in a closed system. Structures and their progression of weak majorization including permutations are given in [17]. Here, we show further results of this approach.

As an application of the above-mentioned mathematical concepts, we use fast decaying liquid foams in the present work. There are several methods to describe foams: measurement of foam volume, bubble interaction like coalescence, gas exchange between bubbles, and pressure differences between the inside and outside of a bubble (Young-Laplace law), collapse of bubbles, and definition of the geometry of bubbles (Plateau laws [18]). Some methods were used in former papers [16, 17, 19].

In this paper, we give a general approach to describe the dynamics of complex systems, like a fast decaying foam, by order structures which are based on the development of distributions.

Foam structures were produced by frothing up with ultrasound (Ultrasonik 28x; NEY) 20 mL of nonfoamed beer (*Haake Beck*) in a rectangular glass vessel (2.5 cm × 20 cm × 2.5 cm) at a temperature of 24 ± 1°C. Pictures were taken at five-second intervals with a CV-M10 CCD-camera with a telecentric lens (JENmetar^{TM}1×/12LD). For illumination, a cold light source (KL 2500 LCD) was used. The position of the camera was at the 22 mL mark of the rectangular vessel, the image size was 6.4 mm by 5 mm (Figure 1).

The foam decay could not only be measured by the decreasing foam volume but also by the decreasing number of bubbles in the foam images. The number of bubbles was found to decrease monotonously over time [17]; see Figure 2.

2. The foam experiment

Each bubble diameter was measured and ten bubble-size intervals defined. Thus we obtained time series of bubble-size distributions with absolute values of the number of bubbles of one-size interval denoted by $F = \{f(t) = (s_i(t))\}$ with $\sum_{i=1}^{10} s_i(t) \geq \sum_{i=1}^{10} s_i(t+1)$ and the corresponding normalized bubble-size distributions, $H = \{h(t) = (p_i(t))\}$ with $\sum_{i=1}^{10} p_i(t) = 1$. The set F can also be normalized to the first bubble-size distribution with the maximum number of bubbles to obtain

$$1 = \sum_{i=1}^{10} \frac{s_i(t_0)}{\sum_{i=1}^{10} s_i(t_0)}, \qquad 1 \geq \sum_{i=1}^{10} \frac{s_i(t)}{\sum_{i=1}^{10} s_i(t_0)} \geq \sum_{i=1}^{10} \frac{s_i(t+1)}{\sum_{i=1}^{10} s_i(t_0)}. \tag{2.1}$$

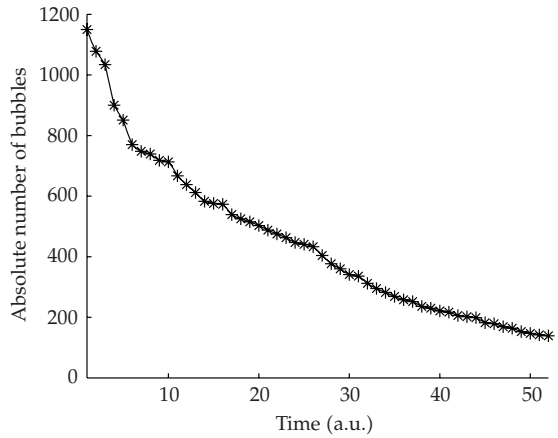

Figure 2: The monotonously decreasing number of bubbles of the foam pictures.

Table 1: The number of intervals i and their interval sizes to obtain bubble-size distributions. As an example, the data of the bubble image in Figure 1 are given: the absolute number of bubbles s_i and the relative frequencies p_i. Note that the last interval is open.

Interval i	Interval size [μm]	No. of bubbles s_i	Relative frequency p_i
1	0–86	98	0.426
2	86–172	46	0.200
3	172–258	29	0.126
4	258–344	18	0.078
5	344–430	11	0.048
6	430–516	13	0.057
7	516–602	4	0.017
8	602–688	3	0.013
9	688–774	4	0.017
10	774–	4	0.017

In Table 1, the bubble-size distribution of the image in Figure 1 is given.

In a former paper [17], we used the same experimental conditions but the area imaged by the camera and the diameter used for bubble-size distribution were larger by a factor of 4 respectively 2, that is the image size was 1.3 cm by 1.0 cm and the corresponding interval size was 173 μm, with images taken every 10 seconds. Consequently, comparison to earlier results allows an assessment of the influence of size and time scale.

3. Concepts of majorization

In the following, we briefly introduce the concepts of classical (Section 3.1) and weak majorizations (Section 3.2). These concepts form the basis of our investigations. In Section 3.3, the discrete majorization is derived from number theory and lattice theory and is extended by a special case of majorization that is based on permutations. A restricted dynamics that underlies majorization will be presented in Section 3.4.

3.1. Classical majorization

Classical majorization belongs to order theory and is a partial order [7]. Comparing two distribution vectors by means of classical majorization, one can distinguish both in terms of statistics. Let $h(t) = (p_i(t))$ and $h(t+1) = (p_i(t+1))$ be two distribution vectors which are normalized to unity, $\sum_{i=1}^{n} p_i(t) = \sum_{i=1}^{n} p_i(t+1) = 1$. To define the relative statistical order between both distribution vectors, one has to sort the vector entries (relative frequencies) in decreasing order and calculate the partial sum vectors $\widetilde{h}(t)$ and $\widetilde{h}(t+1)$. By a greater relation, the partial sum vectors can be compared componentwise as follows:

$$h(t) = \begin{pmatrix} 0.8 \\ 0.1 \\ 0.1 \end{pmatrix}, \qquad \widetilde{h}(t) = \begin{pmatrix} 0.8 \\ 0.8 + 0.1 \\ 0.8 + 0.1 + 0.1 \end{pmatrix} = \begin{pmatrix} 0.8 \\ 0.9 \\ 1 \end{pmatrix}, \tag{3.1}$$

$$h(t+1) = \begin{pmatrix} 0.6 \\ 0.2 \\ 0.2 \end{pmatrix}, \qquad \widetilde{h}(t+1) = \begin{pmatrix} 0.6 \\ 0.8 \\ 1 \end{pmatrix} \begin{matrix} < \\ < \\ = \end{matrix} \begin{pmatrix} 0.8 \\ 0.9 \\ 1 \end{pmatrix} = \widetilde{h}(t). \tag{3.2}$$

In (3.2), one sees the partial sum vector comparison by the greater relation in the last term. In this case, the greater relation is preserved and distribution vector $h(t)$ majorizes distribution vector $h(t+1)$, denoted by $h(t) \succ h(t+1)$, or in other words the transition from $h(t)$ to $h(t+1)$ characterizes a process of decreasing statistical order.

In general, classical majorization can be expressed as follows [7]: let $h(p_i(t))$ and $h(p_i(t+1)) \in \mathbb{R}^n$ be two vectors the entries of which are sorted in decreasing order, $p_1 \geq p_2 \geq \cdots \geq p_n$. Then

$$h(t) \succ h(t+1) \tag{3.3}$$

if

$$\sum_{1}^{k} p_i(t) \geq \sum_{1}^{k} p_i(t+1), \quad k = 1, \ldots, n-1, \tag{3.4}$$

$$\sum_{i=1}^{n} p_i(t) = \sum_{i=1}^{n} p_i(t+1). \tag{3.5}$$

Considering positive semidefinite distribution vectors with $n \geq 3$, incomparableness can occur which is characteristic for a partial order. Incomparableness mathematically means that the greater relation does not persist for increasing k; see (3.6). Such relations are denoted by $h(t) \not\succ h(t+1)$ and $h(t) \not\prec h(t+1)$, abbreviated by $h(t) \times h(t+1)$. This phenomenon of incomparable distributions and their significance for process dynamics will be discussed in Section 4,

$$h(t) = \begin{pmatrix} 0.6 \\ 0.2 \\ 0.2 \end{pmatrix}, \qquad h(t+1) = \begin{pmatrix} 0.5 \\ 0.5 \\ 0 \end{pmatrix}, \qquad \widetilde{h}(t) = \begin{pmatrix} 0.6 \\ 0.8 \\ 1 \end{pmatrix} \begin{matrix} > \\ < \\ = \end{matrix} \begin{pmatrix} 0.5 \\ 1 \\ 1 \end{pmatrix} = \widetilde{h}(t+1). \tag{3.6}$$

3.2. Weak majorization

Classical majorization is applicable to closed systems; see (3.5). A process which is characterized by a loss or a gain of objects can be described by weak majorization [7].

First, we consider a loss of objects, the *weak submajorization*. Then for the distribution vectors of an open system with sink we have

$$\sum_{i=1}^{n} s_i(t) \geq \sum_{i=1}^{n} s_i(t+1). \tag{3.7}$$

The statistical evaluation by weak submajorization works the same as in classical majorization. One sorts the entries in decreasing order and compares the partial sum vectors componentwise.

In general, weak submajorization can be expressed as follows [7]: let $f(t) = (s_i(t))$ and $f(t+1) = (s_i(t+1)) \in \mathbb{R}^n$ be two vectors the entries of which are sorted in decreasing order, $s_1 \geq s_2 \geq \cdots \geq s_n$. Then $f(t)$ weakly submajorizes $f(t+1)$, denoted by

$$f(t) \succ_w f(t+1) \tag{3.8}$$

if

$$\sum_{1}^{k} s_i(t) \geq \sum_{1}^{k} s_i(t+1), \quad k = 1, \ldots, n-1, \tag{3.9}$$

and the relation (3.7) holds.

Both classical majorization and weak submajorization allow incomparableness. Note that because of (3.7) the classical majorization is contained in the weak submajorization, that is, if $h(t)$ majorizes $h(t+1)$, $h(t) \succ h(t+1)$, then $h(t)$ also weakly submajorizes $h(t+1)$, $h(t) \succ_w h(t+1)$. But we like to distinguish both cases because of (3.7) and (3.5) by using the different notations $\succ$ and $\succ_w$. In (3.10) and (3.11), two distribution vectors $f(t)$ and $f(t+1)$ are given. The sums of their entries are different, $\sum_{i=1}^{n} s_i(t) = 1$ and $\sum_{i=1}^{n} s_i(t+1) = 0.9$; see (3.7). We call the entries of distribution vectors with $\sum_{i=1}^{n} s_i < 1$ *weak frequencies*. The derivation of such distributions is shown in Section 2. As an example in (3.11), the greater relation is preserved and therefore vector $f(t)$ weakly submajorizes $f(t+1)$, $f(t) \succ_w f(t+1)$. Such a transition can be characterized by diffusion and sink, but both are weighted in quite different ways:

$$f(t) = \begin{pmatrix} 0.6 \\ 0.2 \\ 0.2 \end{pmatrix}, \qquad f(t+1) = \begin{pmatrix} 0.5 \\ 0.2 \\ 0.2 \end{pmatrix}, \tag{3.10}$$

$$\widetilde{f}(t) = \begin{pmatrix} 0.6 \\ 0.8 \\ 1 \end{pmatrix} > \begin{pmatrix} 0.5 \\ 0.7 \\ 0.9 \end{pmatrix} = \widetilde{f}(t+1). \tag{3.11}$$

An example of incomparableness of the weak submajorization is given in (3.12) and (3.13). The greater relation is not preserved and so neither $f(t)$ weakly submajorizes $f(t+1)$

nor $f(t)$ is weakly submajorized by $f(t+1)$, denoted by $f(t) \not\prec_w f(t+1)$ and $f(t) \not\succ_w f(t+1)$, abbreviated by $f(t) \times f(t+1)$,

$$f(t) = \begin{pmatrix} 0.6 \\ 0.2 \\ 0.2 \end{pmatrix}, \qquad f(t+1) = \begin{pmatrix} 0.7 \\ 0.1 \\ 0.1 \end{pmatrix}, \tag{3.12}$$

$$\tilde{f}(t) = \begin{pmatrix} 0.6 \\ 0.8 \\ 1 \end{pmatrix} \begin{matrix} < \\ > \\ > \end{matrix} \begin{pmatrix} 0.7 \\ 0.8 \\ 0.9 \end{pmatrix} = \tilde{f}(t+1). \tag{3.13}$$

The *weak supermajorization* is defined by the componentwise comparison of partial sum vector entries the original entries of which are rearranged in increasing order, $s_1 \leq s_2 \cdots \leq s_n$. Then $f(t)$ weakly supermajorizes $f(t+1)$,

$$f(t) \succ^w f(t+1) \tag{3.14}$$

if

$$\sum_1^k s_i(t) \leq \sum_1^k s_i(t+1), \quad k = 1, \ldots, n. \tag{3.15}$$

3.3. Discrete majorization

To define discrete majorization, we have to combine number theory with order theory. One important topic in number theory is integer partitions which were first studied by Euler [20, 21]. For many years, one of the most intriguing and difficult questions about them was how to determine the asymptotic properties of the number of partitions of an integer $p(n)$ as n gets large. This question was finally answered by Hardy et al. [22, 23].

A partition of an integer n is a representation of this integer as a sum of natural numbers; examples for partitions of $n = 6$ are given as follows:

$$6, \qquad 5+1, \qquad 4+2, \qquad 4+1+1, \qquad 3+3, \ldots, \qquad 1+1+1+1+1+1. \tag{3.16}$$

Each partition of n can be represented by a Young diagram [13, 14]: there are n boxes and each term of the partition can be assigned to a row of the diagram; see Figure 3. The set of the partitions of n can be represented as vectors which are embedded in the n-dimensional vector space by extending the partition terms with zeros, shown as follows:

$$\begin{pmatrix} 6 \\ 0 \\ 0 \\ 0 \\ 0 \\ 0 \end{pmatrix}, \begin{pmatrix} 5 \\ 1 \\ 0 \\ 0 \\ 0 \\ 0 \end{pmatrix}, \begin{pmatrix} 4 \\ 2 \\ 0 \\ 0 \\ 0 \\ 0 \end{pmatrix}, \begin{pmatrix} 4 \\ 1 \\ 1 \\ 0 \\ 0 \\ 0 \end{pmatrix}, \begin{pmatrix} 3 \\ 3 \\ 0 \\ 0 \\ 0 \\ 0 \end{pmatrix} \cdots \begin{pmatrix} 1 \\ 1 \\ 1 \\ 1 \\ 1 \\ 1 \end{pmatrix}. \tag{3.17}$$

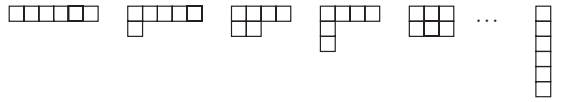

Figure 3: The Young diagrams of the partitions in (3.16).

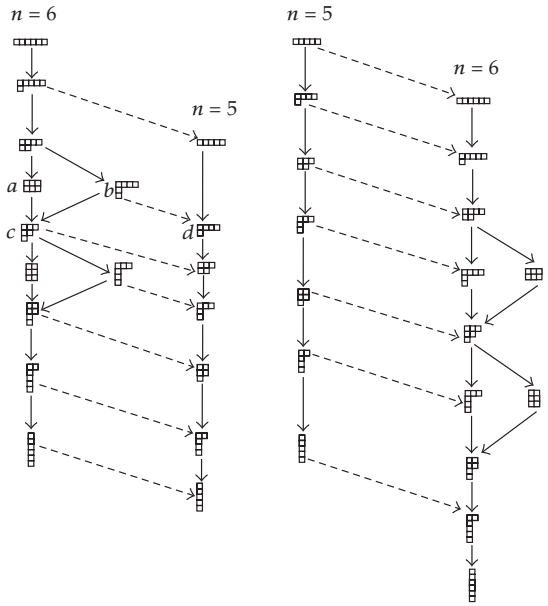

Figure 4: (Left) Two Ruch lattices to show the order of discrete majorization. The arrows show the direction from the least upper bound to the greatest lower bound and characterize the discrete classical majorization. The dashed arrows between both lattices describe the weak submajorization [17]. The diagrams a and b characterize incomparableness in terms of classical majorization and the diagrams c and d incomparableness of the weak submajorization. (Right) The same Ruch lattices, but the dashed arrows represent the weak supermajorization.

All diagrams (or partitions or partition vectors) are comparable by majorization and form lattices. These diagram lattices and the idea to use them for process description go back to Ruch [15]. In Figure 4, the totally ordered $n = 5$ diagram lattice and the partially ordered $n = 6$ diagram lattice are given. Incomparableness of the discrete classical majorization occurs for lattices with $n \geq 6$. One pair of incomparable diagrams of the $n = 6$ lattice is labeled as a and b on the left. Weak majorization can be combined with diagram lattices. In contrast to the arrows which show the direction from the least upper bound to the greatest lower bound and represent the classical majorization ("$\rightarrow$" means $\succ$), the dashed arrows between the lattices on the left correspond to the weak submajorization ("$\rightarrow$" means $\succ_w$); see Figure 4. An example for incomparableness in terms of weak submajorization is given by diagrams c and d. The dashed arrows between the lattices on the right correspond to the weak supermajorization, ("$\rightarrow$" means $\succ^w$). Additionally, by application of the different concepts of weak majorization the order of the diagrams changes; see Figure 4.

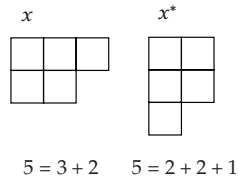

Figure 5: The Young diagram x and its dual diagram $x^{\star}$.

The order of weak majorization is connected by dual diagrams (dual partitions). A dual diagram labeled with an asterisk is the diagram obtained by reflecting the Young diagram along the main diagonal—an exchange of rows and columns; see Figure 5. It holds for the corresponding dual diagrams that if x weakly submajorizes y, $x \succ_w y$, then the dual diagram of y weakly supermajorizes the dual diagram of x, $y^{\star} \succ^w x^{\star}$. Additionally, there is an algorithm to describe the progression of the diagrams from the least upper bound to the greatest lower bound. Note that the rules for classical majorization were given by Ruch [15],

(1) *a diagram with n boxes containing only one box in the lowest occupied row weakly submajorizes a diagram with $n-1$ boxes by eliminating this one box* [17].

Due to the dual diagrams, the weak supermajorization obeys the rule,

(2) *a diagram with n boxes, always containing boxes in the first row, weakly supermajorizes an $n+1$ diagram by gaining one box in the first row.*

Note that these structures are transitive. It holds that if

$$x \succ y, \quad y \succ_w z, \quad \text{then } x \succ_w z, \tag{3.18}$$

and if

$$x \succ_w y, \quad y \succ z, \quad \text{then } x \succ_w z. \tag{3.19}$$

In an analogous manner, (3.18) and (3.19) hold for weak supermajorization.

Additionally, there exists a special case of majorization, *perm(utation)-majorization*, which is based on classical and weak majorizations but the rearrangement of the vector entries is omitted and the set of permutations is taken into account [17]. For weak perm-supermajorization, the permutations can be compared by changing the entry sequence, $s_1 \to s_n$, $s_2 \to s_{n-1}, \ldots, s_n \to s_{n-(n-1)} = s_1$. Then the partial sum comparison follows. The progression of the structures which is constructed by perm-majorization (we called these structures *p*artition-*p*ermutation-structures) without changing the number of boxes is described in [16],

(3) *from any row i containing at least one box, one box shifts to the next row $i+1$.*

If x weakly perm-submajorizes y, x perm $\succ_w y$, then

(4) *only boxes of the last possible row can be eliminated.*

Note that this expression is not identical with the algorithm for weak submajorization. If x weakly perm-supermajorizes y, x perm $\succ^w y$, then

(5) *only the first row can gain boxes, also if this row contains no box.*

A part of the $n = 4$ pp-structure combined with weak perm-submajorization and weak perm-supermajorization is given in Figure 6. The diagram in Figure 6 top right is an example for the rules (4) and (5) above.

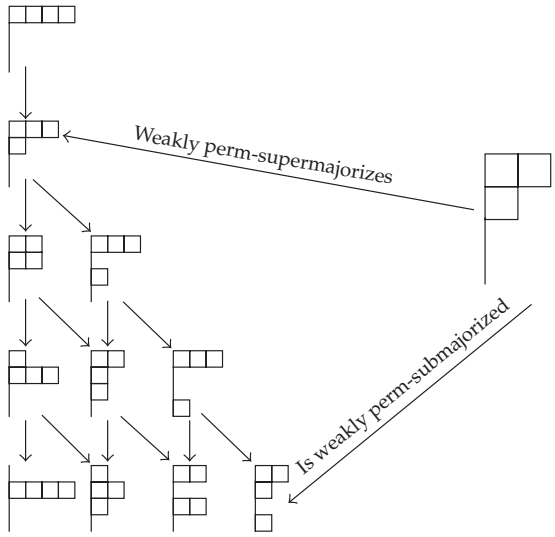

Figure 6: An example for the algorithms 4 and 5.

3.4. Attainability

In [9–12], Zylka described a simple model system in which he considered n bodies (objects), the only property of which is their temperature. Then the system is completely described by a temperature distribution. The process dynamics of these temperature distributions is characterized by a *two-body heat exchange*. That means only two bodies are connected for a period of time and an amount of heat can be transported from the hotter body to the cooler one. Then two other bodies are connected and so on. By this process dynamics, Zylka derived the set of distributions which are attainable from a fixed initial distribution.

We apply this restricted mixing process dynamics to discrete dynamics. Let a Young diagram be characterized by its number of boxes n which are distributed over three rows, then the corresponding diagram vector is $x = (x_i) \in \mathbb{N}^3$ with $x_1 \geq x_2 \geq x_3$ and its trace is defined by $\mathrm{tr}(x) = \sum_{i=1}^{3} x_i = n$. Then the set of attainable diagrams $K(x)$ can be generated by picking two entries x_i, x_j from x with $i < j$. The entry with smaller index i loses boxes, and the other entry j gains boxes as long as $x_i \geq x_j$. Such a transition is denoted by an arrow with (i, j), (i, k), or (j, k) for $i = 1$, $j = 2$, and $k = 3$. An example for the set of attainable diagrams of the initial diagram (6 1 0) is given in Figure 7.

The set $K(x)$ can be ordered by perm-majorization and is represented by a diagram lattice in Figure 8. Let x and x' be two elements of $K(x)$, then the join in the lattice is defined by $x \cup x' = \max(\tilde{x}_j, \tilde{x}'_j)$ and the meet is defined by $x \cap x' = \min(\tilde{x}_j, \tilde{x}'_j)$, where $\tilde{x}$ and $\tilde{x}'$ are the partial sum vectors of x and x'.

4. Majorization as process dynamics

4.1. General

A simple experiment of foam decay exemplifies process dynamics in a statistical sense. The application of majorization to bubble-size distributions is possible if one understands the order

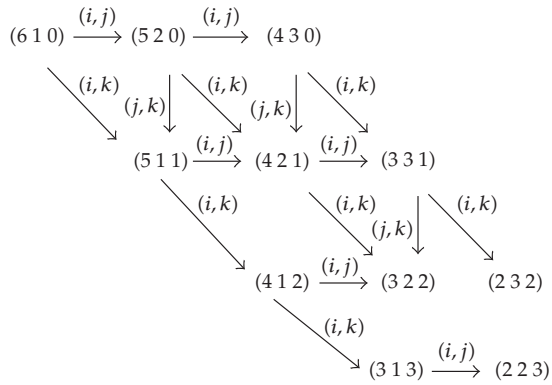

Figure 7: The initial Young diagram (6 1 0) with its set of attainable diagrams. The arrows characterize the individual mixing transitions with the corresponding indices of the diagram vector, $i = 1$, $j = 2$, and $k = 3$.

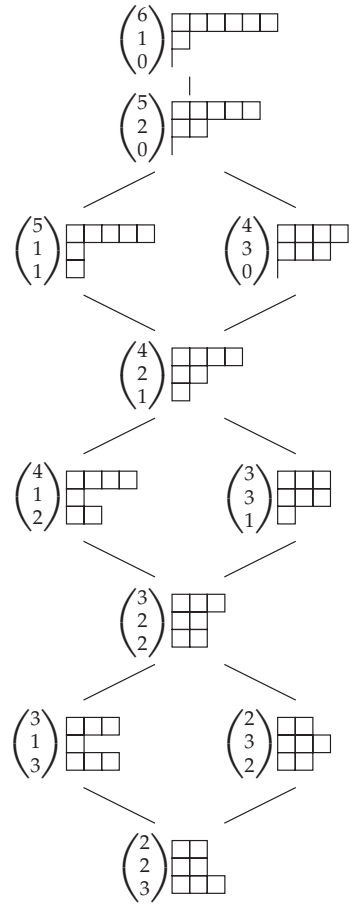

Figure 8: The set $K(x)$ of Figure 7 is ordered by perm-majorization and represented by a diagram lattice.

of majorization as a process dynamics. Hence, let us summarize majorization in words of process dynamics. Now, diagram boxes are objects and rows are states.

Classical majorization

Let us consider an ordinary statistical diffusion process with invariant object number. The attractor of this process is the equal distribution. The problem of incomparableness of classical majorization has not yet been discussed for physicochemical systems. In general, a transition of incomparableness consists at least of two elementary transitions and one of these is inverse. For instance, the transition from diagram a to diagram b (Figure 4) consists of the transitions from diagram a to c and from c to b, $a \succ c$ and $c \prec b$. The second transition is an inverse one. In this case, the inverse transition describes an increasing statistical order. Process dynamics of increasing statistical order leads one to suppose that the process is based on structure formation.

Weak majorization

This concept is subdivided into weak submajorization and weak supermajorization, and contains classical majorization. This relation describes a process of statistical diffusion with noninvariant number of objects. The order of weak submajorization characterizes a diffusion with sink. The sink obeys rule (1), see Section 3.3. The attractor of weak submajorization is the *death* of the system. Incomparableness is given if the statistical order increases and a sink occurs; see the transition from diagram c to diagram d in Figure 4. But also a process of predominating sinks and small sources causes incomparableness. It can be seen that there are more boxes (objects) in the first row of diagram d than in the first row of diagram c. Weak supermajorization leads to a diverging number of objects which are distributed over all states. A diffusion process with source (rule (2)) is described. An increasing statistical order and a source leads to incomparableness. Note that in the presence of sinks and sources, two order structures (weak sub- and supermajorization, resp.) can be assigned to the system. These two order structures (Figure 4) show that incomparable diagrams in terms of weak submajorization are comparable in terms of weak supermajorization and vice versa. In addition, alternating transitions of weak sub- and supermajorization can lead to incomparableness in the classical sense. A simple example is given by

$$\begin{pmatrix} 4 \\ 1 \\ 1 \end{pmatrix} \succ_w \begin{pmatrix} 4 \\ 1 \\ 0 \end{pmatrix} \succ^w \begin{pmatrix} 5 \\ 1 \\ 0 \end{pmatrix} \succ \begin{pmatrix} 4 \\ 2 \\ 0 \end{pmatrix} \succ \begin{pmatrix} 3 \\ 3 \\ 0 \end{pmatrix}, \qquad \begin{pmatrix} 4 \\ 1 \\ 1 \end{pmatrix} \not\succ \begin{pmatrix} 3 \\ 3 \\ 0 \end{pmatrix}, \qquad \begin{pmatrix} 4 \\ 1 \\ 1 \end{pmatrix} \not\prec \begin{pmatrix} 3 \\ 3 \\ 0 \end{pmatrix}. \tag{4.1}$$

The lattices in Figure 4 show this fact clearly.

Permutation-majorization

This concept contains classical and weak majorizations and offers the possibility of multimodal distributions. With a constant object number, the process is defined by rule (3), that is, every object stepwise passes through all states whereby the statistical order can decrease or increase and multimodal distributions are possible. By taking permutations into account, the large increase in the overall number of possible distributions leads to the result that many more states are incomparable; see Figure 6. The process ends if all objects are in the last possible state (lowest row). If the object number decreases, weak perm-submajorization obeys rule (4), that is, an object has to pass through all states (classical perm-majorization) before it leaves the system. The weak perm-supermajorization obeys the process of classical perm-majorization with a source in the first state.

4.2. Foam dynamics

Foam decay can be subdivided into two processes, drainage and rearrangement [16, 17, 19, 24]. Sometimes a third process is mentioned which describes the drying of foam [25]. During ultrasound degassing, only very small bubbles are formed. The corresponding distribution shows a sharp peak. During drainage, the liquid flows out of the foam and the distribution broadens. The rearrangement phase is characterized by processes like coalescence and bursting of bubbles or growing of larger bubbles on cost of smaller ones. During this phase, certain bubble packings can be formed [19, 26].

The bubble-size distributions of our measurements (see Section 2) are ordered by the different concepts of majorization which have been introduced in Section 3. Tables 2 and 3 show these relations, which are denoted by $h(k)Rh(k+1)$ for distributions which are normalized to unity and $f(k)Rf(k+1)$ if a sink is taken into account. R is the relation and $k = t[s]/5s$ describes the time steps. Additionally, we distinguish between five-second intervals, $h(k)Rh(k+1)$ or $f(k)Rf(k+1)$, and ten-second intervals, $h(2k)Rh(2k+2)$ or $f(2k)Rf(2k+2)$, in order to compare the results of [17]. Transitions of incomparableness are denoted by × for all relations.

In the second and third columns of Table 2, the relation of the classical majorization is given. The fourth and fifth columns contain the relation of the weak submajorization. In Table 3, the comparison of the bubble-size distributions by perm-majorization (second and third columns) and weak perm-submajorization (third and fourth columns) is given. We also applied the weak supermajorization and weak perm-supermajorization, running the process backwards.

Classical majorization and its perm-variant

By classical majorization we obtain a partially ordered set of bubble-size distributions in the second and third columns of Table 2. During drainage, transitions of classical majorization predominate, that is, the drainage obeys an ordinary diffusion process. During rearrangement phase, there are a lot of incomparable distributions and inverse transitions of classical majorization, respectively. The incomparableness increases by reducing the time steps. Such transitions of incomparableness characterize an increasing statistical order which can be caused by structure formation. The foam is attracted by a structure (a certain packing of

Table 2: The order of the different concepts of majorization concerning bubble-size distributions is given. One sees the time steps in the first column. The second and third columns show the relation R of classical majorization with different time steps. The transitions of the weak submajorization can be examined in the fourth and fifth columns differing in the time steps. Incomparable distributions are denoted by ×.

$k = t[s]/5s$	$h(k)Rh(k+1)$	$h(2k)Rh(2k+2)$	$f(k)Rf(k+1)$	$f(2k)Rf(2k+2)$
0	$\succ$	$\succ$	$\succ_w$	$\succ_w$
1	$\succ$		$\succ_w$	
2	$\succ$	$\succ$	$\succ_w$	$\succ_w$
3	$\succ$		$\succ_w$	
4	$\succ$	$\succ$	$\succ_w$	$\succ_w$
5	×		$\succ_w$	
6	×	×	$\succ_w$	$\succ_w$
7	×		$\succ_w$	
8	×	$\succ$	×	$\succ_w$
9	$\succ$		$\succ_w$	
10	$\succ$	$\succ$	$\succ_w$	$\succ_w$
11	×		$\succ_w$	
12	×	×	$\succ_w$	$\succ_w$
13	$\succ$		$\succ_w$	
14	×	×	×	$\succ_w$
15	×		$\succ_w$	
16	×	×	×	×
17	×		×	
18	×	×	$\succ_w$	$\succ_w$
19	×		×	
20	×	×	$\succ_w$	$\succ_w$
21	×		$\succ_w$	
22	$\succ$	×	$\succ_w$	$\succ_w$
23	×		×	
24	×	$\succ$	$\succ_w$	$\succ_w$
25	$\succ$		$\succ_w$	
26	×	×	$\succ_w$	$\succ_w$
27	×		$\succ_w$	
28	$\succ$	×	$\succ_w$	$\succ_w$
29	×		×	
30	$\succ$	$\succ$	$\succ_w$	$\succ_w$
31	×		$\succ_w$	
32	×	$\succ$	$\succ_w$	$\succ_w$
33	×		$\succ_w$	
34	×	×	×	$\succ_w$
35	×		$\succ_w$	
36	×	$\succ$	$\succ_w$	$\succ_w$
37	×		$\succ_w$	
38	×	×	$\succ_w$	$\succ_w$
39	$\succ$		$\succ_w$	
40	×	$\succ$	$\succ_w$	$\succ_w$
41	$\succ$		$\succ_w$	

Table 2: Continued.

$k = t[s]/5s$	$h(k)Rh(k+1)$	$h(2k)Rh(2k+2)$	$f(k)Rf(k+1)$	$f(2k)Rf(2k+2)$
42	×	×	×	$\succ_w$
43	×		$\succ_w$	
44	×	×	$\succ_w$	$\succ_w$
45	×		$\succ_w$	
46	×	×	$\succ_w$	$\succ_w$
47	×		$\succ_w$	
48	$\succ$	$\succ$	$\succ_w$	$\succ_w$
49	×		$\succ_w$	
50	×		×	

different sized bubbles) which cannot be attained because a loss of bubbles predominates. This supports the results of the former paper [17]. Incomparableness can also be the result of sources and sinks. The two incomparable distributions in (3.12) give an example. That means the loss of bubbles predominates, see Figure 2, but there can still be sources of small bubbles even in the rearrangement phase either by formation of small bubbles out of the liquid or by the collapse of larger bubbles.

It is very interesting that the order structure of our measurement is comparable to the measurements of [17], but the behavior of the Shannon entropy [27],

$$I(h) = \frac{1}{\log_2 n} \sum_{i=1}^{n} p_i, \tag{4.2}$$

shows no process separation; see Figure 9. Our current measurement shows an approximately increasing Shannon entropy. The measurement of [17] was described by an increasing Shannon entropy during drainage and a decreasing and increasing (*zig-zag* behavior) entropy during rearrangement. This supports the assumption of an inhibited structure formation. It is possible that the reduction of the image size leads to an increasing statistical influence of small bubbles. The large number of small bubbles predominates the statistics. The maximum value of the Shannon entropy is approximately 0.28. In [17], the maximum value is 0.64. The high frequency of the first bubble size class of our current measurement inhibits an increase of the entropy measure.

Application of classical perm-majorization (Table 3, second and third columns) leads to an increase of incomparableness in comparison to classical majorization. Additionally, the incomparableness increases from 10-second time steps to 5-second time steps. An increase of incomparable distributions by changing from classical majorization to classical perm-majorization is also given by [17]. In contrast to the current measurement, the total order during drainage is preserved in both classical majorization and classical perm-majorization referring to [17].

The increase of incomparableness in terms of classical perm-majorization depends on the fact that the omission of the rearrangement of the vector entries leads to an influence of certain bubble-size classes, that is, not only the relative frequencies independent of bubble-size class influence the partial sum comparison, but also both of the relative frequency and the corresponding bubble-size class. By classical perm-majorization, weighting for bubble-size classes is introduced.

Table 3: The evaluation of the different concepts of perm-majorization. In the first column the time steps are given. One sees the relation R of the perm-majorization in the second column and the weak perm-submajorization in the third column. Incomparableness are denoted by $\times$.

$k = t[s]/5s$	$h(k)Rh(k+1)$	$h(2k)Rh(2k+2)$	$f(k)Rf(k+1)$	$f(2k)Rf(2k+2)$
0	perm $\succ$	perm $\succ$	perm $\succ_w$	perm $\succ_w$
1	perm $\succ$		perm $\succ_w$	
2	perm $\succ$	perm $\succ$	perm $\succ_w$	perm $\succ_w$
3	$\times$		perm $\succ_w$	
4	$\times$	perm $\succ$	perm $\succ_w$	perm $\succ_w$
5	$\times$		$\times$	
6	$\times$	$\times$	perm $\succ_w$	perm $\succ_w$
7	$\times$		perm $\succ_w$	
8	$\times$	perm $\succ$	$\times$	perm $\succ_w$
9	$\times$		perm $\succ_w$	
10	$\times$	perm $\succ$	perm $\succ_w$	perm $\succ_w$
11	$\times$		perm $\succ_w$	
12	$\times$	$\times$	perm $\succ_w$	perm $\succ_w$
13	$\times$		perm $\succ_w$	
14	$\times$	$\times$	$\times$	perm $\succ_w$
15	$\times$		perm $\succ_w$	
16	$\times$	$\times$	$\times$	$\times$
17	$\times$		$\times$	
18	$\times$	$\times$	perm $\succ_w$	perm $\succ_w$
19	$\times$		$\times$	
20	$\times$	$\times$	perm $\succ_w$	perm $\succ_w$
21	$\times$		perm $\succ_w$	
22	$\times$	$\times$	perm $\succ_w$	perm $\succ_w$
23	$\times$		$\times$	
24	$\times$	perm $\succ$	perm $\succ_w$	perm $\succ_w$
25	$\times$		perm $\succ_w$	
26	$\times$	$\times$	perm $\succ_w$	perm $\succ_w$
27	$\times$		perm $\succ_w$	
28	$\times$	$\times$	perm $\succ_w$	perm $\succ_w$
29	$\times$		$\times$	
30	$\times$	$\times$	perm $\succ_w$	perm $\succ_w$
31	$\times$		perm $\succ_w$	
32	$\times$	perm $\succ$	perm $\succ_w$	perm $\succ_w$
33	$\times$		perm $\succ_w$	
34	$\times$	$\times$	$\times$	perm $\succ_w$
35	$\times$		perm $\succ_w$	
36	$\times$	$\times$	perm $\succ_w$	perm $\succ_w$
37	$\times$		perm $\succ_w$	
38	$\times$	$\times$	perm $\succ_w$	perm $\succ_w$
39	$\times$		perm $\succ_w$	
40	$\times$	perm $\succ$	perm $\succ_w$	perm $\succ_w$
41	$\times$		perm $\succ_w$	
42	$\times$	$\times$	$\times$	perm $\succ_w$

Table 3: Continued.

$k = t[s]/5s$	$h(k)Rh(k+1)$	$h(2k)Rh(2k+2)$	$f(k)Rf(k+1)$	$f(2k)Rf(2k+2)$
43	×		perm $\succ_w$	
44	×	×	×	perm $\succ_w$
45	×		perm $\succ_w$	
46	×	×	perm $\succ_w$	perm $\succ_w$
47	×		perm $\succ_w$	
48	×	×	perm $\succ_w$	perm $\succ_w$
49	×		perm $\succ_w$	
50	perm $\succ$		×	

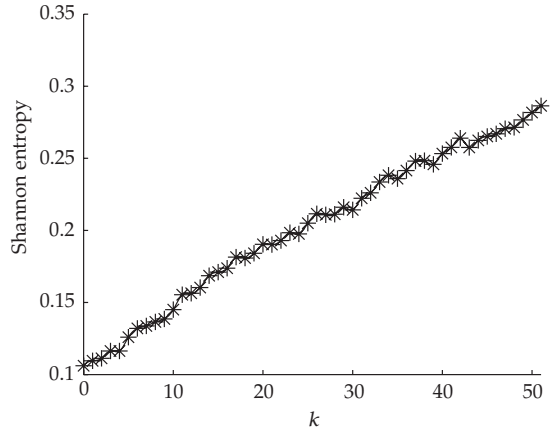

Figure 9: The Shannon entropy development of the bubble-size distribution set H.

Weak submajorization and its perm-variant

Both weak submajorization and weak perm-submajorization show only few incomparable distributions. The incomparableness increases by reducing the time steps; see the fourth column in Tables 2 and 3. The order structure (practically a total order) of the fifth column in Table 2 and Table 3 is also given by the measurement of [17]. In terms of weak submajorization, both measurements obey a diffusion process with a sink which occurs if a bubble belonging to the next vicinal-size class has formed. This dynamics would allow for bubbles of all sizes but the smallest one to be eliminated. In contrast, weak perm-submajorization only allows a bubble of the largest possible size to disappear, which may, therefore, be the realistic concept for sinks in systems where a critical size is required for elimination. Additionally, foam decay obeys the complicated diffusion process defined by rule (3).

Since the number of bubbles is monotonously decreasing, see Section 2, the few transitions of incomparableness (fourth column in Tables 2 and 3) could be related to a source of a certain bubble-size class or an increasing statistical order. Probably, within ten seconds the sink predominates in such a manner that diffusion processes or a small source cannot be taken into account by weak submajorization and weak perm-submajorization. In summary, the order

structures in terms of weak submajorization and weak perm-submajorization seem to be time-step-variant, but image size-invariant.

Weak supermajorization and its perm-variant

Applying weak supermajorization and weak perm-supermajorization, the bubble-size distributions of all measurements are incomparable with very few exceptions.

These results are easy to understand. If the weak submajorization and the weak perm-submajorization show an approximately total order, the inversion of these orders can lead to incomparableness in terms of weak supermajorization and weak perm-supermajorization. In other words, the inversion of a statistical diffusion (decreasing statistical order) with sink is an increasing statistical order with source, respectively incomparableness. This inversion seems also to be valid for the weak perm-submajorization and weak perm-supermajorization. Note that the source occurs in the first size class. Therefore, only small bubbles are formed by running the process backwards. These order structures seem to be independent of time and image-size scale.

Attainability

By the concept of attainability, a two-body dynamics is described which is based on equalizing processes. Zylka described a two-body heat exchange [9–12], but instead of bodies and their temperature we consider bubble-size classes and their relative frequencies.

In [16, 24], we showed the approximate *oscillating* behavior of individual bubble sizes. In the beginning, the first size class decreases and the vicinal-size class increases. Both size classes obey an equalizing process until the next size class appears which grows on cost of one or of both of the other classes. This behavior exactly corresponds to the process dynamics of Zylka. Indeed, the set of the bubble-size distributions is in the set of attainable distributions starting from the first bubble-size distribution.

The fact that the set of our bubble-size distributions H is attainable starting from the first distribution means that the statistical dynamics of the bubble sizes obeys an exchange of two size classes concerning the relative frequency. Now it would be interesting to investigate an exchange between three or more size classes.

For the set of bubble-size distributions F there does not exist a concept of attainability, a kind of *weak attainability* taking sources or sinks into account. To introduce a source or sink can depend on the original set of attainability $K(x)$ or on the elements of that set. Let us consider the first possibility for the introduction of a sink by the concept of weak perm-submajorization. One generates the set of $K(x)$ and picks out of this set the diagram of the highest order x' that can obey algorithm (4); see Section 3.3. After eliminating a box of the lowest row, $x'\text{perm} \succ_w y$, the set of attainability $K_1(y)$ can be generated. Both sets, $K(x)$ and $K(y)$, would represent the set of weak attainability.

The other possibility is that one picks out of set $K(x)$ all diagrams which can obey algorithm (4). The resulting diagrams would represent the set $K_2(y)$. The number of diagrams of the set $K_1(x)$ does not equal $K_2(x)$. In an analogous manner, a source can be introduced. Still both concepts of weak attainability have to be investigated in detail in terms of consistency and application to process dynamics in future work.

5. Discussion

The change of the time steps from 10 to 5 seconds particularly influences the order structures of the normalized bubble-size distributions by an increasing number of incomparable bubble-size distributions. In contrast, for the order structures of the variants of weak majorization including permutations, the reduction of the time steps leads to a marginal change since only a few incomparable distributions occur additionally. Also the reduction of the image size is only of significance for the normalized bubble-size distributions. The corresponding order structures of classical majorization and classical perm-majorization are preserved but the time development of the Shannon entropy (4.2), see Figure 9, changes conspicuously. Instead of a process separation [17], an approximately monotonous function behavior is given which is caused by the strong influence of the smallest bubble-size class. Note that although this function behavior is given, the distributions are predominantly incomparable. The other order structures are not influenced by changing the image size with the exception of the order structure of weak supermajorization which shows a slight increase of incomparableness by the size reduction.

For the set of normalized bubble-size distributions, further investigations concerning the dependency of order structures on the time scale (time steps) are important. The question is whether a further reduction of the time steps leads to an increase of incomparableness or shows a loss of incomparable distributions but a gain of transitions of decreasing $h(t) \succ h(t+1)$ or increasing $h(t) \prec h(t+1)$ statistical order.

Provided that the reduction of the time interval leads to incomparableness of normalized bubble-size distributions and does not change the comparable distributions in terms of weak submajorization, then one has to define transitions for which it holds that $f(t) \succ_w f(t+1)$ and the same distributions are incomparable in terms of classical majorization:

$$(411000) \succ_w (320000) \tag{5.1}$$

$$\text{but } 1/6(411000) \not\succ 1/5(320000), \tag{5.2}$$

$$1/6(411000) \not\prec 1/5(320000). \tag{5.3}$$

But a further transition of decreasing order, $(320000) \succ (311000)$, leads to two comparable pairs of distributions in terms of both classical and weak submajorizations:

$$(411000) \succ_w (311000), \tag{5.4}$$

$$1/6(411000) \succ 1/5(311000). \tag{5.5}$$

It is also possible that there is a transition of weak submajorization and the transition of the same normalized distributions is of increasing order:

$$(411000) \succ_w (410000), \tag{5.6}$$

$$1/6(411000) \prec 1/5(410000). \tag{5.7}$$

Let transitions consist of a part of sink and a part of *entropy distance*, which characterizes the relative difference of statistical entropy between the compared distributions. Since the sink of

the examples above is constant, the statistical order decreases from (410000) to (320000) to (311000):

$$(410000) \succ (320000) \succ (311000), \tag{5.8}$$

and hence the entropy distance to the initial distribution (411000) increases; one may say that for the transition (5.1) the sink and the entropy distance are relatively balanced, but for (5.4) the entropy distance is greater and for (5.6) is less.

If the incomparableness increases by diminishing the time intervals, the decaying foam would be a regular diffusion process with a sink. In case that the temporal reduction leads to transitions of decreasing $h(t) \succ h(t+1)$ or increasing $h(t) \prec h(t+1)$ statistical order in terms of classical majorization and the total order of weak submajorization is preserved, the examples of (5.4)–(5.7) describe the experimentally observed development of the bubble-size distributions. Then the foam decay process would be characterized by phases of predominating diffusion or sink. For our foam statistics, it is of high importance to understand how the sink and the diffusion are connected.

The evaluation of the order structures of decaying foam by normalized bubble-size distributions shows interesting results like process separation [17] and sets of attainability, but this concept is problematic and, respectively, it is dependent on certain conditions like time and image-size scales. Additionally, one has to take into account that this system is open and that normalization emphasizes certain bubble-size classes according to the image size. Therefore, normalization may misrepresent the statistics, since the number of bubbles decreases.

6. Outlook

Characterization of processes by order structures can in general lead to an understanding of the transitions allowed in a system and the states which are attainable from initial conditions without specifying any kinetics, assigning transition probabilities, or explicitly running simulations. While classical majorization is appropriate for closed systems, the occurrence of sinks or sources can be described by weak sub- or supermajorization, respectively. The inclusion of permutations makes sure that sinks can only occur in the last row (weak perm-submajorization). Sources can only enter in the first row whether permutations are included or not. This is not only realistic for the example described (foam dynamics), but for any system in which small nuclei form (1st row), then grow (while moving downward), and finally leave the system when they become too large. This is the case, for example, for precipitation reactions or water droplets forming in the atmosphere, or more generally for any process which can meaningfully be divided into discrete steps and has clearly defined sources and sinks (say raw material and finished product).

The advantage of order structures is therefore that they can be used to classify a large class of systems. However, it is only possible to determine which states are attainable, not which will actually be reached. Since there is no explicit time dependence, it can in the presence of sinks and sources not even be determined whether an attractor exists (let alone what it would look like). To this end, a specific kinetics has to be assumed (resp., transition probabilities assigned for stochastic models). Obviously a large variety of different kinetics can be defined on a given order structure depending on the system(s) under consideration. In most cases, one would expect to reach a stationary state, but also oscillatory behavior is

possible (e.g., if larger particles grow faster and the reaction velocities depend on (at least) one additional variable, such as monomer concentration or degree of supersaturation) [28, 29]. Despite these limitations, we believe that order structures may be a valuable (additional) tool for the abstract characterization of processes also in open systems. It could be possible in the future to determine basic properties of a given system by assigning it to certain types of order structures.

Acknowledgments

The authors like to thank Uwe Sydow for helpful discussions and Katharina Knicker for the measurements.

References

[1] G. Hardy, J. Littlewood, and G. Pólya, *Inequalities*, Cambridge University Press, London, UK, 1934.
[2] R. Muirhead, "Some methods applicable to identities and inequalities of symmetric algebraic functions of n letters," *Proceedings of the Edinburgh Mathematical Society*, vol. 21, pp. 144–157, 1903.
[3] A. Uhlmann, "Sätze über Dichtematrizen," *Wissenschaftliche Zeitschrift der Karl-Marx-Universität Leipzig. Mathematisch-Naturwissenschaftliche Reihe*, vol. 20, pp. 633–637, 1971.
[4] A. Uhlmann, "Endlich-dimensionale Dichtematrizen. I," *Wissenschaftliche Zeitschrift der Karl-Marx-Universität Leipzig. Mathematisch-Naturwissenschaftliche Reihe*, vol. 21, pp. 421–452, 1972.
[5] P. M. Alberti and A. Uhlmann, *Dissipative Motion in State Spaces*, vol. 33 of *Teubner-Texte zur Mathematik*, B. G. Teubner, Leipzig, Germany, 33rd edition, 1981.
[6] P. M. Alberti and A. Uhlmann, *Stochasticity and Partial Order: Doubly Stochastic Maps and Unitary Mixing*, vol. 9 of *Mathematics and Its Applications*, D. Reidel, Dordrecht, The Netherlands, 1982.
[7] A. W. Marshall and I. Olkin, *Inequalities: Theory of Majorization and Its Applications*, vol. 143 of *Mathematics in Science and Engineering*, Academic Press, New York, NY, USA, 1979.
[8] M. A. Nielsen, *Quantum information theory*, Ph.D. thesis, University of New Mexico, Albuquerque, NM, USA, 1998.
[9] C. Zylka, *Zur Erreichbarkeit von Zuständen bei Ausgleichsvorgängen*, Ph.D. thesis, Sektion Physik, Universität Leipzig, Leipzig, Germany, 1982.
[10] C. Zylka, "A note on the attainability of states by equalizing processes," *Theoretical Chemistry Accounts*, vol. 68, no. 5, pp. 363–377, 1985.
[11] C. Zylka, "Eine Verallgemeinerung des Satzes von Muirhead," *Wissenschaftliche Zeitschrift der Karl-Marx-Universität Leipzig. Mathematisch-Naturwissenschaftliche Reihe*, vol. 34, no. 6, pp. 598–601, 1985.
[12] C. Zylka, "Zum Problem der Erreichbarkeit von Zuständen," *Annalen der Physik*, vol. 499, no. 3, pp. 247–248, 1987.
[13] A. Young, "On quantitative substitutional analysis," *Proceedings of the London Mathematical Society*, vol. 33, no. 1, pp. 97–145, 1901.
[14] A. Young, *The Collected Papers of Alfred Young (1873–1940)*, Mathematical Expositions no. 21, University of Toronto Press, Toronto, Canada, 1977.
[15] E. Ruch, "The diagram lattice as structural principle," *Theoretical Chemistry Accounts*, vol. 38, no. 3, pp. 167–183, 1975.
[16] S. Sauerbrei and P. J. Plath, "Diffusion without constraints," *Journal of Mathematical Chemistry*, vol. 42, no. 2, pp. 153–175, 2007.
[17] S. Sauerbrei, K. Knicker, E. C. Haß, and P. J. Plath, "Weak majorization as an approach to non-equilibrium foam decay," *Applied Mathematical Sciences*, vol. 1, no. 9–12, pp. 527–550, 2007.
[18] J. A. F. Plateau, *Statique Expérimentale et Théorique des Liquides soumis aux seules Forces Moléculaires, Vol. 2*, Gauthier-Villars, Paris, France, 1873.
[19] S. Sauerbrei, E. C. Haß, and P. J. Plath, "The Apollonian decay of beer foam bubble size distribution and the lattices of Young diagrams and their correlated mixing functions," *Discrete Dynamics in Nature and Society*, vol. 2006, Article ID 79717, 35 pages, 2006.

[20] L. Euler, *Introduction to Analysis of the Infinite. Book I*, Springer, New York, NY, USA, 1988.
[21] G. E. Andrews, *The Theory of Partitions*, Cambridge Mathematical Library, Cambridge University Press, Cambridge, UK, 1998.
[22] G. H. Hardy and S. Ramanujan, "Asymptotic formulaæ in combinatory analysis," *Proceedings of the London Mathematical Society*, vol. 17, no. 1, pp. 75–115, 1918.
[23] H. Rademacher, "On the partition function $p(n)$," *Proceedings of the London Mathematical Society*, vol. 43, no. 4, pp. 241–254, 1937.
[24] S. Sauerbrei, U. Sydow, and P. J. Plath, "On the characterization of foam decay with diagram lattices and majorization," *Zeitschrift für Naturforschung A*, vol. 61, no. 3-4, pp. 153–165, 2006.
[25] C. Dale, C. West, J. Eade, M. Rito-Palomares, and A. Lyddiatt, "Studies on the physical and compositional changes in collapsing beer foam," *Chemical Engineering Journal*, vol. 72, no. 1, pp. 83–89, 1999.
[26] D. Weaire and S. Hutzler, *The Physics of Foams*, Oxford University Press, Oxford, UK, 1999.
[27] C. E. Shannon, "A mathematical theory of communication," *The Bell System Technical Journal*, vol. 27, pp. 379–423, 623–656, 1948.
[28] M. B. Rubin, R. M. Noyes, and K. W. Smith, "Gas-evolution oscillators. 9. A study of the ammonium nitrite oscillator," *Journal of Physical Chemistry*, vol. 91, no. 6, pp. 1618–1622, 1987.
[29] K. Bar-Eli and R. M. Noyes, "Gas-evolution oscillators. 10. A model based on a delay equation," *Journal of Physical Chemistry*, vol. 96, no. 19, pp. 7664–7670, 1992.